ELSEVIER

Journal of Structural Geology 29 (2007) 629–645

JOURNAL OF STRUCTURAL GEOLOGY

www.elsevier.com/locate/jsg

Development of lattice preferred orientation in clinoamphiboles deformed under low-pressure metamorphic conditions. A SEM/EBSD study of metabasites from the Aracena metamorphic belt (SW Spain)

M. Díaz Aspiroz [a,*], G.E. Lloyd [b], C. Fernández [c]

[a] *Dpto. Sistemas Físicos, Químicos y Naturales, Universidad Pablo de Olavide, Crtra, Utrera, km 1, 41013 Seville, Spain*
[b] *School of Earth & Environment, The University, Leeds LS2 9JT, UK*
[c] *Departamento de Geodinámica y Paleontología, Facultad de Ciencias Experimentales, Universidad de Huelva, Campus de El Carmen, 21071 Huelva, Spain*

Received 24 May 2006; received in revised form 29 September 2006; accepted 27 October 2006
Available online 27 December 2006

Abstract

The mechanical properties of the lower continental crust are intimately related to the rheology of calcic clinoamphibole. Naturally deformed clinoamphibole typically shows brittle behaviour under a wide range of deformation conditions, whereas crystal plasticity is rarely observed. In this study, the microfabric of clinoamphiboles from metabasites deformed under low-pressure/medium-to-high temperature metamorphic conditions is presented. Amphiboles from all samples have developed LPO that can be attributed to different deformation mechanisms depending on deformation temperature, fluid content, structure and phase-strength contrasts. Rigid body rotation of amphibole prisms within a weaker plagioclase matrix corresponds to metabasites deformed under medium deformation temperatures that show a weak layer structure and a high phase strength-contrast between plagioclase and clinoamphibole. Lower temperatures and the presence of fluids mean that one of the studied rocks was affected also by dissolution-precipitation creep and cataclastic flow. In the final sample, dislocation creep was accommodated by recovery and subgrain rotation dynamic recrystallization in monominerallic hornblende layers at higher temperatures, which could be representative of the rheology of amphiboles in a lower continental crust at high temperature conditions.

Keywords: Cataclastic flow; High-temperature deformation; Misorientation; Phase-strength contrast; Rigid body rotation; Subgrain rotation dynamic recrystallization

1. Introduction

The mechanical behaviour of the lower continental crust, which is closely related to the formation and evolution of crustal-scale structures (e.g., Wilks and Carter, 1990), is considered to be basically controlled by polyphase rocks composed primarily of plagioclase and hornblende (e.g., Kirby and Kronenberg, 1987; Ranalli and Murphy, 1987). Whilst the behaviour of plagioclase is relatively well-known (e.g., Stünitz and Fitz Gerald, 1993; Rybacki and Dresen, 2004; Terry and Heidelbach, 2006), a better knowledge of the rheology of calcic amphibole is crucial in improving understanding of the mechanical properties of the lower continental crust. Furthermore, some physical properties of this part of the lithosphere (namely, seismic lamination and seismic anisotropy) are intimately related to the lattice preferred orientation (LPO) of anisotropic minerals (e.g., Mainprice et al., 2000; Meissner et al., 2006 and references therein), with hornblende being perhaps the most important phase.

Calcic clinoamphiboles are thought to be one of the strongest lower crustal minerals (e.g., Brodie and Rutter, 1985; Shelley, 1994). Nevertheless, there is significant disagreement on the mechanisms taking place during hornblende deformation.

* Corresponding author. Tel.: +34 9 5434 8351; fax: +34 9 5434 9151.
E-mail address: mdiaazp@upo.es (M. Díaz Aspiroz).

0191-8141/$ - see front matter © 2006 Elsevier Ltd. All rights reserved.
doi:10.1016/j.jsg.2006.10.010

Experimentally deformed clinoamphiboles under very high strain rates typically show $(\bar{1}01)$ mechanical twinning, together with (100)[001] dislocation glide without dynamic recrystallization (Rooney et al., 1970, 1975; Dollinger and Blacic, 1975; Morrison-Smith, 1976). However, these deformation mechanisms are likely to play a role in naturally deformed amphiboles only under extreme deformation conditions, such as shock-loaded rocks (Chao, 1967). Additionally, under high temperature conditions, dislocation glide, incipient dynamic recrystallization and fracturing have also been reported (Hacker and Christie, 1990). In contrast, naturally deformed amphiboles typically show brittle behaviour, sometimes along with solution mass transfer, under low greenschists to amphibolites facies conditions (Allison and La Tour, 1977; Brodie and Rutter, 1985; Nyman et al., 1992; Lafrance and Vernon, 1993; Stünitz, 1993; Babaie and La Tour, 1994; Berger and Stünitz, 1996; Kruse and Stünitz, 1999; Imon et al., 2004), as well as (100) mechanical twinning at temperatures ranging from 350 to 540 °C (Dollinger and Blacic, 1975; Biermann, 1981; Cumbest et al., 1989). Kinking has been reported only rarely (Imon et al., 2004; Baratoux et al., 2005). Crystal plasticity has been observed occasionally for temperatures ranging from 450 to >650 °C, including dynamic (although usually chemically enhanced) recrystallization (Cumbest et al., 1989), dislocation creep on (100)[001] (Skrotzki, 1992) and subgrain formation by dislocation glide on (hk0)[001] (Biermann and van Roermund, 1983). Finally, deformation by dissolution-precipitation creep under upper greenschist – lower amphibolite facies conditions has been described in amphibolites from the Ryoke Belt (Imon et al., 2002).

In this study, LPO of calcic amphiboles from the Aracena metamorphic belt (SW Spain) are analysed. These amphiboles are found in metabasites (amphibolites and mafic schists) that were deformed under low-pressure metamorphic conditions ($P < 6$ kbar), at temperatures ranging from 650 °C to 970 °C.

2. Geological setting

The Aracena metamorphic belt (AMB) is a long and narrow band located at the contact between the Ossa-Morena zone (OMZ) and the South-Portuguese zone (SPZ), two of the main units forming part of the Iberian Massif (SW European Variscan Chain). The limits of the AMB lie parallel to the main regional structures, which trend in a WNW-ESE direction. According to the division proposed by Castro et al. (1999), two domains can be distinguished in the AMB: an oceanic domain (OD) to the south and a continental domain (CD) to the north (Fig. 1). In the northern part of the OD, the Acebuches metabasites are in contact with the CD. The Acebuches metabasites were derived, according to various geochemical studies, from the high-temperature/low-pressure (HT/LP) metamorphism of former oceanic crust with MORB affinities (Bard and Moine, 1979; Dupuy et al., 1979; Quesada et al., 1994; Castro et al., 1996).

The Acebuches metabasites were affected, during the Variscan orogeny, by three main tectono-metamorphic events (Castro et al., 1996; Díaz Aspiroz and Fernández, 2005). The first stage involved a HT/LP metamorphic event (AM-M_1), which reached the amphibolite-granulite facies transition, along with a ductile shear deformation (AM-D_1). Subsequently, the structural base of the Acebuches metabasites was affected by a retrometamorphism (AM-M_2) related to a mylonitic deformation (AM-D_2). This second deformation event was responsible for the juxtaposition of the Acebuches metabasites onto the Pulo do Lobo accretionary prism, through the formation and activity of the Southern Iberian shear zone (SISZ) (Crespo-Blanc and Orozco, 1988). The characteristics of the structures generated during AM-D_2 in the SISZ suggest that: (1) the SISZ is an oblique transpressional shear zone with triclinic symmetry (Díaz Aspiroz and Fernández, 2005); and (2) the finite strain was higher toward the structural base of the Acebuches metabasites (Díaz Aspiroz and Fernández, 2003, 2005). Finally, the Calabazares shear zone (AM-D_3) affected the top of the series, at the contact between the Acebuches metabasites and the CD.

The CD is composed of a variety of high and medium grade metamorphic rocks, including schists, gneisses, migmatites, calc-silicates, amphibolites and marbles, as well as various intermediate to basic intrusive rocks (Fig. 1). The El Rellano amphibolites (Castro et al., 1996), which are part of the CD, show cross-cutting relationships with foliated calc-silicate rocks, suggesting an intrusive (gabbroic) origin for these rocks.

The CD underwent, during Variscan plate convergence, a complex tectonic evolution that comprised up to four ductile deformation phases (Díaz Aspiroz et al., 2006). The first stage (CD-D_1) has been traditionally related to km-scale recumbent folds (e.g., Bard, 1969). In the high-grade rocks of the AMB, the CD-S_1 foliation is only preserved within some CD-S_2 foliation microlithons. The second tectonic event (CD-D_2) is associated with widespread extension that caused generalised axial flattening and discrete shear zones with a normal sense of displacement. A penetrative metamorphic foliation (CD-S_2) is present throughout the CD, whereas within shear zones a localized mylonitic foliation (also CD-S_2) and a related stretching lineation (CD-L_2) have developed. This deformation phase was accompanied by a high-temperature/low-pressure (HT/LP) metamorphism that affected the CD (Díaz Aspiroz et al., 2006). The third stage (CD-D_3) generated symmetric upright folds with variable fold axial trace orientations but only in some minor fold hinges in the marbles has a weak axial-planar foliation (CD-S_3) developed (Díaz Aspiroz et al., 2003). The last ductile deformation event (CD-D_4) resulted in km-scale, SW-verging antiforms and several reverse shear zones. A penetrative mylonitic foliation (CD-S_4) and a related stretching lineation (CD-L_4) developed within these shear zones.

3. Rock types and samples

According to their structural features, the Acebuches metabasites can be divided into two main groups (Fig. 1, Table 1): (1) banded amphibolites that were unaffected by AM-D_2 and show therefore structures formed only by AM-D_1; and (2) mylonitic metabasites that were affected by AM-D_2 (Díaz Aspiroz and Fernández, 2005). The banded amphibolites

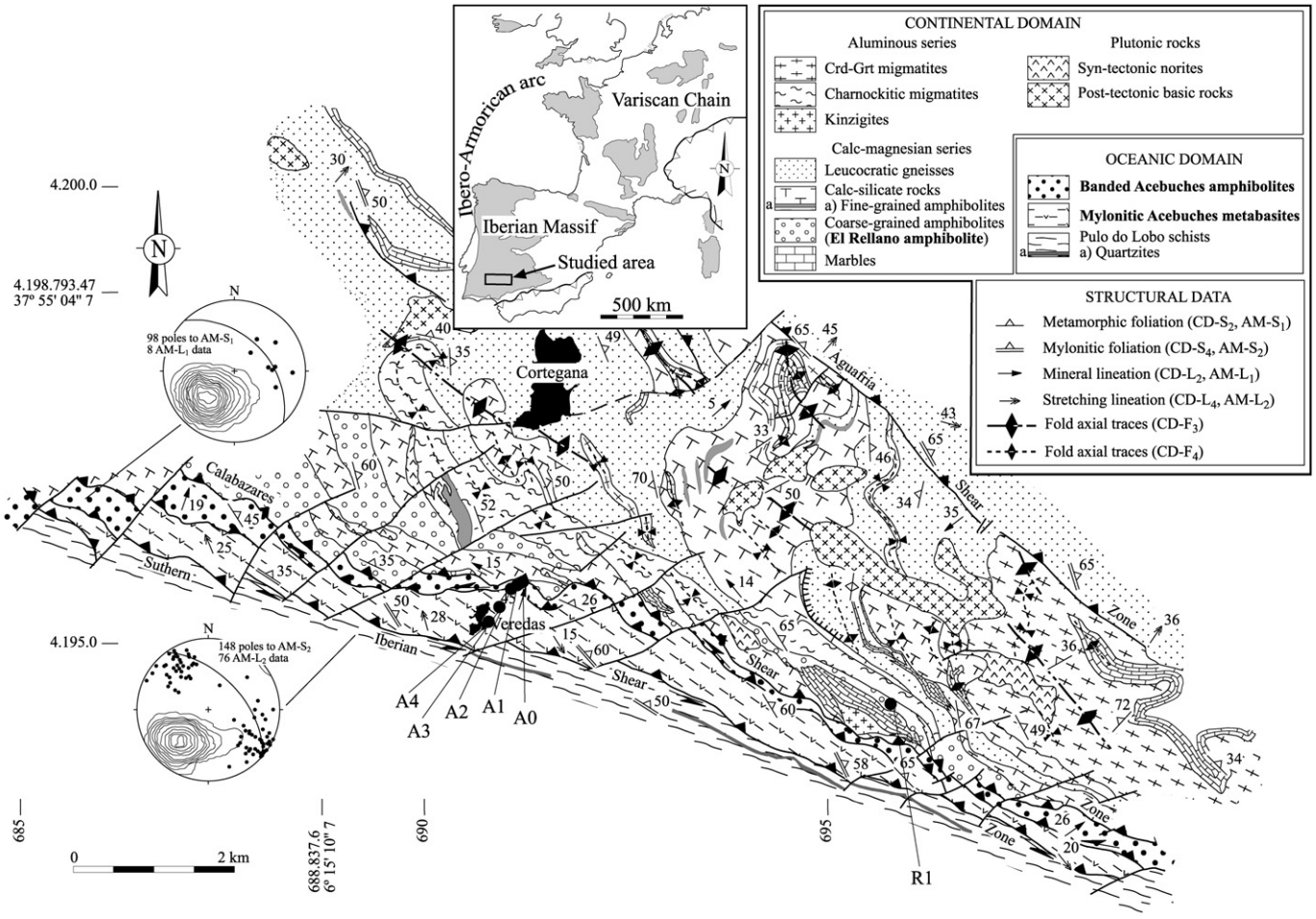

Fig. 1. Geological map of the Aracena Metamorphic Belt (after Díaz Aspiroz et al., 2006) with lower hemisphere, equal-area projections of: (1) poles to AM-S_1 and AM-S_2 and average foliation planes; and (2) AM-L_1 and AM-L_2. Studied rock types appear in bold and specific sample locations are shown. Inset is a general map of the European Variscan Chain with the location of the studied area. Geographical and UTM (zone S-29, data in km) coordinates are shown for reference.

can be further subdivided into two metamorphic facies, clinopyroxene-bearing (Pl-Hb-Cpx) coarse-grained banded amphibolites and clinopyroxene-lacking (Pl-Hb) medium-grained banded amphibolites. Similarly, the mylonitic metabasites can be subdivided also into mylonitic amphibolites (with Pl-Hb assemblages) and mylonitic mafic schists (with Pl-Hb-Act-Ep-Chl assemblages). The El Rellano amphibolites are mainly composed of plagioclase, hornblende and diopside. These rocks, which show a pegmatitic isotropic texture elsewhere in the CD, were locally affected by a ductile CD-D_4 shear zone that generated a typical mylonitic texture.

Six samples of different metabasites from the AMB have been collected for this study. Five of these samples (A0 to A4) correspond to the Acebuches metabasites and are located on the Veredas cross-section (see Fig. 1 for location). They represent a complete section across the Acebuches metabasites unit, with well documented data on grain size and grain shape (Díaz Aspiroz and Fernández, 2003) and mineral chemistry and thermometry (Díaz Aspiroz, 2006; Díaz Aspiroz et al., 2006). In detail, sample A0 is a Cpx-bearing coarse-grained banded amphibolite, samples A1 and A2 are Pl-Hb medium-grained banded amphibolites, sample A3 is a mylonitic amphibolite and sample A4 is a mylonitic mafic schist. Only one sample of the mylonitic El Rellano amphibolite (R1) has been collected (see Fig. 1 for location). However, due to significant chemical and textural differences between hornblende porphyroclasts cores and mantle grains, they may be distinguished as R1-Por and R1-Mant. A summary of the main features of the metabasites studied in this work is shown in Table 1.

3.1. Microfabric description

Apart from a brief microfabric description (Fig. 2), some grain size and shape preferred orientation (SPO) data are presented. Length of the long and short axes of amphibole grains were measured on XZ sections (normal to the foliation and parallel to the lineation) under an optical microscope using the software Finite Strain Tensor (FIST, Dias, 2004), and the aspect ratio (R) was calculated from these data. The measuring procedure is described in detail by Díaz Aspiroz and Fernández (2003). The orientation of the long axis with respect to the foliation trace (angle ϕ) was measured also (anticlockwise positive − clockwise negative) and represented against the

Table 1
Main features of the samples: TME, tectono-metamorphic event registered by the sample; grain size and aspect ratio data of samples A0–A5 from Díaz Aspiroz and Fernández (2003); temperatures calculated from Hb-Pl thermometer (Holland and Blundy, 1994) at 4 kbar and represent highest temperature registered by each sample

Sample	A0	A1	A2	A3	A4	R1-Por	R1-Mant
Rock	Acebuches metabasites					El Rellano amphibolite	
	Banded amphibolites			Mylonitic metabasites			
	Cpx-bearing	Cpx-lacking		Amphibolite	Mafic schist		
Main mineral assemblage	Pl + Hb + Di ± Qtz	Pl + Hb ± Qtz			Pl + Hb + Act ± Qtz ± Ep ± Chl	Hb + Pl + Di	
Pl/Hb (mode)	61/39	57/43	53/47	67/33	59/41	37/63	
TME	AM-D_1-M_1			AM-D_2-M_2		CD-D_4	
Am grain-size	300 μm–1.5 cm	100–500 μm		50–150 μm	10–100 μm	400 μm–2 cm	15–400 μm
Am aspect ratio	1–3	1–3		2–7	2–10	1–3	
Foliation	Grain-size layering Metamorphic			Mylonitic		Pl-Hb layering Mylonitic	
Lineation	Mineral (rare)	–		Stretching/Mineral		Stretching	
Temp. (°C) ± 40	825	770	750	720	655	970	840

aspect ratio in Fig. 3. A detailed grain-size analysis of the Acebuches metabasites is presented by Díaz Aspiroz and Fernández (2003).

The Acebuches banded amphibolites (samples A0 to A2) show a penetrative cm- to dm-scale grain-size layering parallel to a weak metamorphic foliation (AM-S_1) defined by the preferred orientation of hornblende blasts (Fig. 2a). The grain-size layering is more pronounced in the coarse-grained amphibolites (sample A0, grain size ranges from 300 μm to 1.5 cm, Table 1) compared with the medium-grained amphibolites (samples A1 and A2, grain size ranges from 100 to 500 μm, Table 1). The difference in grain size between both facies depends on the presence or absence of the coarse-grained layers (Díaz Aspiroz and Fernández, 2003). In both cases, the hornblendes appear as subhedral prisms with a small aspect ratio in the XZ section (1–3, Figs. 2a,b and 3a, Table 1) and define, together with tabular plagioclase blasts, a granoblastic texture (Fig. 2b). Hornblende, plagioclase and diopside may appear also as rotated porphyroblasts wrapped by AM-S_1. The hornblende grains do not show any intragranular microstructures indicative of crystal plastic deformation (i.e. undulose extinction, deformation lamellae, subgrain boundaries, bulging, etc.). Rather, they exhibit weak fracturing but no other brittle deformation features (i.e. irregularly-shaped subgrains, domino structures, etc.) have been found (Fig. 2b).

The Acebuches mylonitic metabasites (samples A3 and A4) are characterised by a penetrative foliation (AM-S_2) defined by the preferred orientation of prismatic amphibole blasts with large aspect ratios (ranging from 2 to 7 in the amphibolites and from 2 to 10 in the mafic schists, Figs. 2c,d and 3b, Table 1) and, in the mafic schists, by epidote + chlorite-rich layers. A lineation defined by plagioclase ribbons and the preferred orientation of amphibole prisms is observed on the foliation planes. Grain size is fine to very fine decreasing progressively towards the structural base of the SISZ (i.e., 50–150 μm in the amphibolites and 10–100 μm in the mafic schists, Table 1). The coarsest grains correspond to rotated porphyroclasts that appear wrapped by AM-S_2 (Fig. 2c,d). In the mylonitic metabasites, amphiboles do not show any crystal plastic deformation features but display intense fracturing suggesting cataclastic deformation. Fractures develop parallel to (100) and (010) planes (Fig. 2c,d) and normal to the [001] axis (Fig. 3e).

The El Rellano amphibolite (sample R1) exhibits a compositional layering defined by plagioclase-rich and hornblende-rich bands (Fig. 2f), which probably resulted from grain-size reduction of the parental pegmatitic gabbro. In either layer, the dominant phase represents more than 90% of the modal composition. A lineation defined preferentially by plagioclase ribbons is observed on the foliation planes. Plagioclase layers are composed of very fine polygonised grains that surround very scarce isolated fine-grained porphyroclasts (Fig. 2f). These features suggest that plagioclase has been almost completely recrystallized. Hornblende layers show porphyroclasts displaying a core and mantle structure (Fig. 2f–h). Cores are medium-to-coarse-grained (grain sizes ranging from 400 μm to 2 cm, Table 1) have small aspect ratios (1–3, Figs. 2f and 3c, Table 1) and often exhibit undulose extinction (Fig. 2g) and bent cleavage planes (Fig. 2h). The orientation of most hornblende porphyroclasts defines a positive angle (preferentially around 30°) with respect to the layering plane (Fig. 3c). These porphyroclasts rotated in an anticlockwise sense could be defining C′-planes. Mantles form polygonised aggregates of regularly-shaped subgrains and grains with a uniform, very fine, size (grain sizes from 5 to 400 μm, Table 1); a small aspect ratio (1–3, Fig. 3d, Table 1) and straight or slightly curved boundaries (Fig. 2g). These grains are not preferentially oriented (Fig. 3d). Subgrain boundaries at the margin of the cores are optically distinguishable and a gradual transition from subgrain aggregates to mantle grains aggregates is observed (Fig. 2g). A lateral transition from subgrains boundaries into higher angle mantle grain boundaries also occurs (Fig. 3g,h).

3.2. P-T conditions

As stated above, three different metamorphic facies can be distinguished in the Acebuches metabasites according to their mineral assemblages (Table 1): (1) the Cpx-bearing

coarse-grained amphibolites reached the upper amphibolite-lower granulite facies transition; (2) The Cpx-lacking medium-grained amphibolites and the mylonitic amphibolites reached the amphibolite facies; and (3) the mafic schists deformed under lower amphibolite-greenschists facies transition. The presence of diopside in the mineral assemblage of the El Rellano amphibolite (Table 1), which appears to be in textural equilibrium with plagioclase and hornblende (porphyroclasts and mantle grains), indicates that this rock reached the upper amphibolite-lower granulite facies transition and maintained these conditions at least during the first stages of CD-D_4.

The P-T conditions during deformation of the studied amphiboles have been further constrained using amphibole mineral chemistry (Table 2 and Fig. 4) and thermometry (Table 1). The analyses were performed on polished, carbon-coated thin sections, by Energy Dispersive Spectrometry (EDS) using a LINK-ISIS system on a JEOL-JSM 5410 SEM at the University of Huelva (Spain). Operating conditions were a probe current of 3.8 nA and an accelerating voltage of 15 kV. Analytical routines included ZAF correction procedures (three iterations) based on standards defined by a combination of pure metals, oxides and minerals.

The amphibole composition of the banded amphibolites in the Acebuches metabasites (samples A0 to A2) is somewhat different from that of the mylonitic metabasites (samples A3 and A4), as shown in Table 2 and Fig. 4a. In the former, amphiboles show a consistent Mg-hornblende composition, with no differences between granoblastic grains from the matrix and porphyroblasts. In the latter, amphiboles display a much wider compositional range from hornblende (*s.l.*) to actinolite in the mafic schists, although Mg-hornblende compositions predominate. Compositional ranges in the Acebuches metabasites amphiboles are due mainly to variations in Si and A-site occupancy (Table 2, Fig. 4a) which are more important in the mylonitic metabasites (Si (p.f.u.) = 6.71–7.94, $(Na + K)^A$ = 0–0.46) than in the banded amphibolites (Si (p.f.u.) = 6.54–7.37, $(Na + K)^A$ = 0.16–0.44). In both cases, amphiboles are enriched in Mg with respect to Fe (Mg# = 0.60–0.75 and 0.45–0.82, respectively). In the El Rellano amphibolites, alkali-rich calcic amphiboles (mainly pargasite and, to a lesser amount, edenite) predominate (Table 2, Fig. 4a). A few grains from the mantle of porphyroclasts show Mg-hornblende composition.

Variations in amphibole composition in the Aracena metamorphic belt metabasites may be attributed mainly to changes in the P-T conditions (e.g., Castro et al., 1996). These variations can be considered in terms of coupled substitutions into the additive component tremolite (Spear, 1981), and their relative importance have been broadly evaluated using two diagrams displayed in Fig. 4b,c. A plot of Al^{iv} vs. $Al^{vi} + Fe^{3+} + Ti + (Na + K)^A$ (Fig. 4b) shows a linear correlation that intercepts the origin, suggesting that the studied amphiboles meet the ideal substitution mechanism proposed by Robinson et al. (1971). Thus, Al^{vi}, Fe^{3+} and Ti in the octahedral sites, together with the A-site occupancy, are balanced by Al^{iv} substituting Si in the tetrahedral sites by means of the edenite, tschermakite, Fe-tschermakite, Ti-tschermakite and pargasite substitutions, which are all temperature-sensitive (e.g., Grapes and Graham, 1978; Spear, 1981; Blundy and Holland, 1990). From this, it is deduced that these cations could not be involved in other substitutions such as glaucophane, riebeckite and richterite (see Blundy and Holland, 1990), which therefore remained inactive. Such substitutions are sensitive to pressure (e.g., Grapes and Graham, 1978; Spear, 1981). A poor correlation that deviates from a 1:1 line in a Na^{M4} vs Al^{vi} plot (Fig. 4c) also supports the low activity of the glaucophane substitution. In consequence, it can be suggested that the observed compositional variability in amphiboles from the AMB were due mainly to changes in temperature, whereas pressure remained constant at low values. The preference of Al for the tetrahedral sites over the octahedral sites (Table 2, see also Díaz Aspiroz, 2006) is also indicative of low-pressure metamorphism (e.g., Spear, 1993). Furthermore, according to the calibration by Brown (1977), the Na^{M4} content in the studied amphiboles suggests that pressure was lower than 4 kbar (Fig. 4c). Pressure estimations based on the quartz-jadeite equilibrium in quartz-bearing amphibolites of the Acebuches metabasites (Castro et al., 1996) as well as barometric calculations in metapelites outcropping near the El Rellano amphibolites (Díaz Aspiroz et al., 2006) also point to low-pressure metamorphic conditions for the Aracena metamorphic belt.

Comparative qualitative temperature estimations can be performed on amphiboles based on the Al^{iv}, Ti and $(Na + K)^A$ content (e.g., Brown, 1977; Grapes and Graham, 1978; Spear, 1981; Blundy and Holland, 1990). Data from the Acebuches metabasites (Fig. 4b, see also Díaz Aspiroz et al., 2006) suggest that temperature decreases along the Veredas cross-section from sample A0 (Cpx-bearing coarse-grained banded amphibolites) to sample A4 (mafic schists). From Fig. 4b it is deduced that: (1) hornblende porphyroclasts from the El Rellano amphibolite (sample R1-Por) formed under extremely high-temperature conditions; and (2) the deformation that generated the mantle grains in this rock (sample R1-Mant) initiated under very high-temperature conditions and probably evolved towards lower (although still high) temperatures with progressive deformation. Temperature calculations using the Hb-Pl thermometer based on the edenite + 4 quartz = tremolite + albite or the edenite + albite = richterite + anorthite equilibria (Holland and Blundy, 1994) further support these observations (Table 1).

4. Petrofabric analysis

The petrofabric of the amphiboles in each sample was determined via electron backscattered diffraction (EBSD) in a CamScan scanning electron microscope (SEM) at the University of Leeds. SEM operating conditions were 20 kV accelerating voltage, ~20 nA specimen current and a working distance of ~40 mm, with specimens tilted at 75°. Each sample was prepared via mechanical and chemical polishing prior to coating with a thin film of carbon deposited by vacuum evaporation (e.g., Lloyd, 1987). Amphibole EBSD patterns were indexed using the Channel 5 software of HKL Technology incorporating specific hornblende compositions crystal

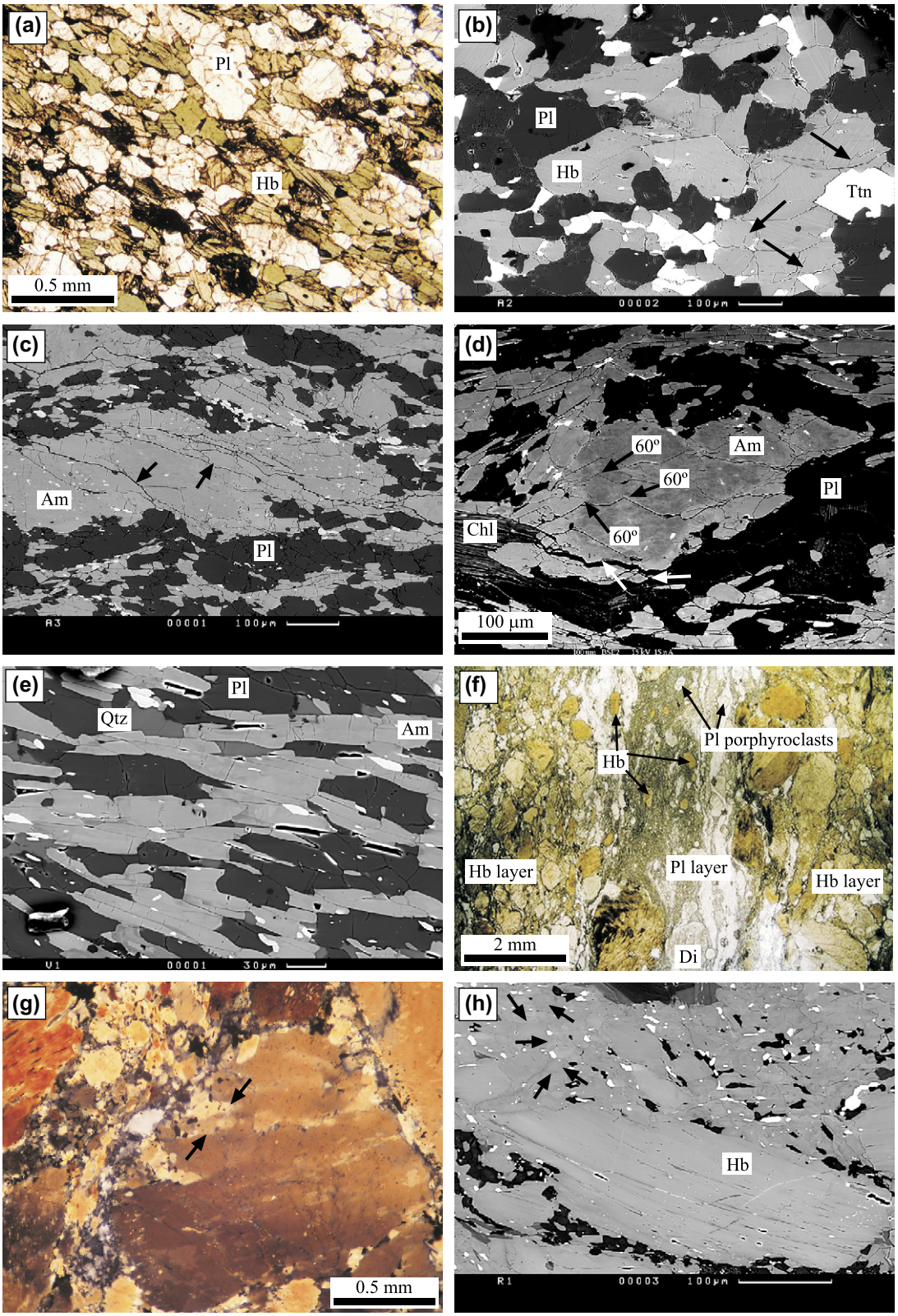

Fig. 2. Microstructures of the studied samples; (a) and (f) are plane polarized light and (g) is crossed polarized light microscope images; (b), (c), (d), (e) and (h) are back scattered electron (BSE) images. Mineral abbreviations after Kretz (1983). (a) Medium-grained banded amphibolite (sample A1) with a weak metamorphic foliation (AM-S_1) defined by the preferred orientation of amphibole blasts. (b) Detailed image of sample A2 showing a granoblastic texture defined by both plagioclase and hornblende (arrows: hornblende blasts with weak fracturing). (c) (hk0) section of intensively fractured hornblende porphyroclast found in mylonitic amphibolite (sample A3). Arrows point to main fractures within the porphyroclast. (d) Mafic schist (sample A4) showing fractured amphibole porphyroclast. Black arrows point to fractures that define 60° angles, which suggests development parallel to (100) and (010) cleavage planes and that the image corresponds to a (001) section of the porphyroclast. White arrows indicate blasts that have been formed from porphyroclasts by means of fracturing. (e) Mafic schist (sample A4) showing

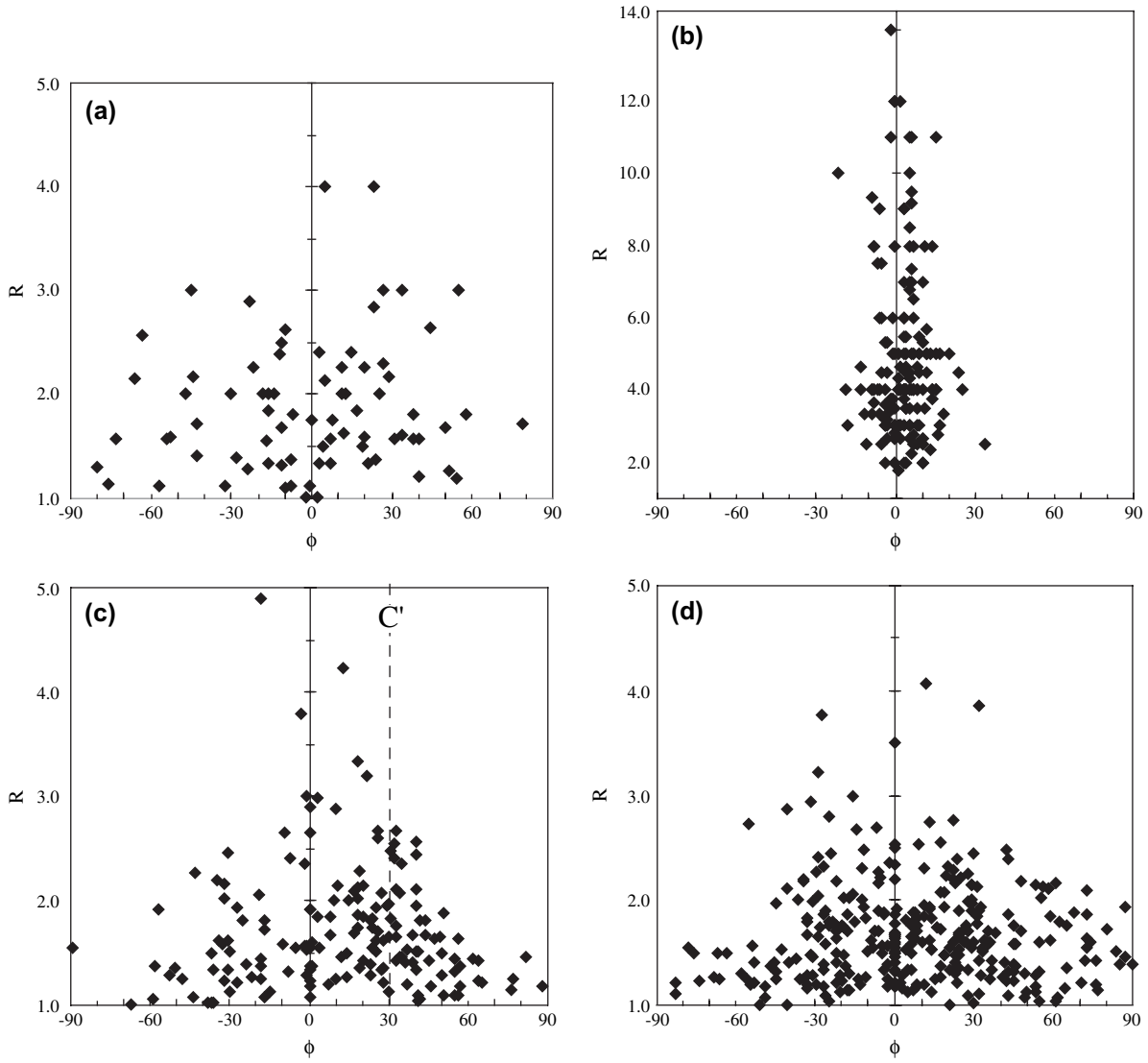

Fig. 3. Amphibole aspect ratios (R) against orientation of long axes from the compositional layering trace (ϕ) measured in the XZ section, being positive when is anticlockwise. (a) Acebuches banded amphibolites (sample A1). (b) Acebuches mylonitic metabasites (mafic schists of sample A4). (c) Porphyroclasts cores of the El Rellano amphibolites (sample R1-Por). C′-planes orientation is depicted with a dashed line. (d) Mantle grains of the El Rellano amphibolites (sample R1-Mant).

files obtained from the UK EPSRC Chemical Database Service (e.g., Fletcher et al., 1996) and the Cambridge Structural Database (e.g., Allen, 2002). The EBSD data were processed in to conventional LPO pole figures for selected crystallographic planes and directions using the program PFch5 (Mainprice, 2003; see also Mainprice, 1990; Mainprice and Humbert, 1994). In addition, misorientation angle distributions and inverse pole (crystal coordinates) figures of misorientation axis/angle pairs between neighbouring grains were derived also using the Channel software.

4.1. LPO

Fig. 5 shows the LPO of the studied samples. In metabasites affected by the SISZ (i.e. samples A3 and A4) the LPO are well-developed and characterised by (100) planes lying parallel to the foliation (XY) planes, (010) planes lying parallel to the XZ plane, which could be interpreted as the vorticity normal section (VNS), and the [001] direction parallel to the X-direction (Fig. 5d,e). These results are in agreement with most published amphibole LPO data obtained using different

intense fracturing normal to the c-axis of elongated amphibole prisms. (f) Compositional layering in the El Rellano amphibolites (sample R1). Hornblende layers show a characteristic core and mantle structure whereas plagioclase appears almost completely recrystallized. (g) Detail of a porphyroclast showing undulose extinction and core and mantle structure. Subgrains boundaries at the core margin are optically distinguishable (arrows) and a gradual transition from aggregates of subgrains (centre) to aggregates of small mantle grains (top-left) is observed. Both subgrains and small mantle grains are of the same size. Subgrains boundaries pass laterally into higher-angle grain boundaries. (h) Hornblende porphyroclast from the El Rellano amphibolite (sample R1) showing bending of cleavage planes and a core and mantle structure. Arrows point to subgrain boundaries in the mantle, which pass laterally into grain boundaries.

Table 2
Representative mineral chemistry analyses of amphiboles calculated via energy dispersive spectrometry (accelerating voltage 15 kV, probe current 3.8 nA): Fe^{3+} estimated using Holland and Blundy (1994); names after Leake, 1997

Sample	A0	A1	A2	A3	A4	R1-Por	R1-Mant
SiO_2	45.03	48.18	49.12	47.93	50.37	42.98	46.49
TiO_2	1.90	1.09	0.65	0.64	0.00	1.20	1.01
AL_2O_3	9.11	6.06	7.04	6.98	3.38	12.48	9.66
Cr_2O_3	0.00	0.00	0.00	0.00	0.41	0.00	0.00
FeO^t	14.00	15.09	12.73	15.91	12.94	11.60	11.35
MnO	0.27	0.00	0.47	0.39	0.33	0.00	0.00
MgO	12.78	14.12	15.54	12.28	14.66	13.03	14.20
CaO	12.12	11.63	10.74	12.02	12.43	12.28	12.47
Na_2O	1.50	1.10	1.34	0.85	0.48	1.99	1.70
K_2O	0.18	0.09	0.00	0.39	0.00	0.61	0.47
Total	**96.89**	**97.36**	**97.63**	**97.39**	**95.00**	**96.17**	**97.35**
Structural formulae in base of 23 oxigens							
Si	6.66	7.02	7.02	7.06	7.48	6.38	6.78
Al^{iv}	1.34	0.98	0.98	0.94	0.52	1.62	1.22
T	**8.00**	**8.00**	**8.00**	**8.00**	**8.00**	**8.00**	**8.00**
Al^{vi}	0.25	0.06	0.21	0.27	0.07	0.56	0.44
Ti	0.21	0.12	0.07	0.07	0.00	0.13	0.11
Cr	0.00	0.00	0.00	0.00	0.05	0.00	0.00
Fe^{3+}	0.30	0.55	0.62	0.32	0.29	0.15	0.06
Mg	2.82	3.07	3.31	2.70	3.24	2.88	3.09
Fe^{2+}	1.43	1.20	0.79	1.64	1.32	1.27	1.30
Mn	0.00	0.00	0.00	0.00	0.03	0.00	0.00
M1–3	**5.00**	**5.00**	**5.00**	**5.00**	**5.00**	**5.00**	**5.00**
Mg	0.00	0.00	0.00	0.00	0.00	0.00	0.00
Fe^{2+}	0.00	0.09	0.11	0.00	0.00	0.02	0.02
Mn	0.03	0.00	0.06	0.05	0.01	0.00	0.00
Ca	1.92	1.82	1.65	1.90	1.98	1.95	1.95
Na	0.04	0.10	0.18	0.05	0.01	0.02	0.03
M4	**2.00**	**2.00**	**2.00**	**2.00**	**2.00**	**2.00**	**2.00**
Na	0.39	0.21	0.19	0.19	0.13	0.55	0.45
K	0.03	0.02	0.00	0.07	0.00	0.12	0.09
A	**0.42**	**0.23**	**0.19**	**0.26**	**0.13**	**0.66**	**0.53**
Ca^{M4}	1.92	1.82	1.65	1.90	1.98	1.95	1.95
Si (p.f.u.)	6.66	7.02	7.02	7.06	7.48	6.38	6.78
Mg#	0.66	0.72	0.81	0.62	0.71	0.69	0.70
$(Na + K)^A$	0.42	0.23	0.19	0.26	0.13	0.66	0.53
Name	Mg-Hb	Mg-Hb	Mg-Hb	Mg-Hb	Mg-Hb	Prg	Ed

techniques (e.g. Siegesmund et al., 1994; Berger and Stünitz, 1996; Egydio-Silva et al., 2002; Imon et al., 2004; Baratoux et al., 2005). The LPO are somewhat better developed as the structural base of the series is approached (i.e., from sample A3 to sample A4).

Amphibole LPO are less well developed and more varied in amphibolites unaffected by the SISZ (i.e. samples A0, A1 and A2; Fig. 5a–c). Although (100) planes lie subparallel to the foliation plane, (010) planes have a range of orientations, including subparallel to the XZ plane (sample A0), occupying a great circle girdle about Z (sample A2), or a nearly random distribution (sample A1). Similarly, The [001] directions show a range of orientations, approaching subparallelism with the X-direction but tending also to define a great circle girdle around Z. These patterns are compatible with field observations of banded amphibolites that rarely or only weakly exhibit a lineation.

Amphiboles from the El Rellano amphibolites (e.g., sample R1) display strong LPO (Fig. 5g), although care must be taken to avoid the biasing effects (see Fig. 5f) of coarse-grained (long axes larger than 5 mm) porphyroclasts that occur in these rocks. The (100) planes define two orientations subparallel to either the foliation plane or the XZ plane. Similar behaviour is shown by the (010) planes, although the data are more dispersed within a great circle girdle slightly inclined with respect to YZ. Irrespective of the precise orientation of the (100) and (010) planes, they combine to produce a strong preferred orientation of the [001] directions slightly inclined in a clockwise sense with respect to the X-direction.

4.2. Misorientation

The misorientation between adjacent crystal lattices separated by a common boundary can be defined either by a simple misorientation angle distribution or more precisely by the lowest rotation angle about a common axis that brings the two lattices in to parallelism (e.g., Randle, 1993; Lloyd et al., 1997). Both misorientation angle distributions and

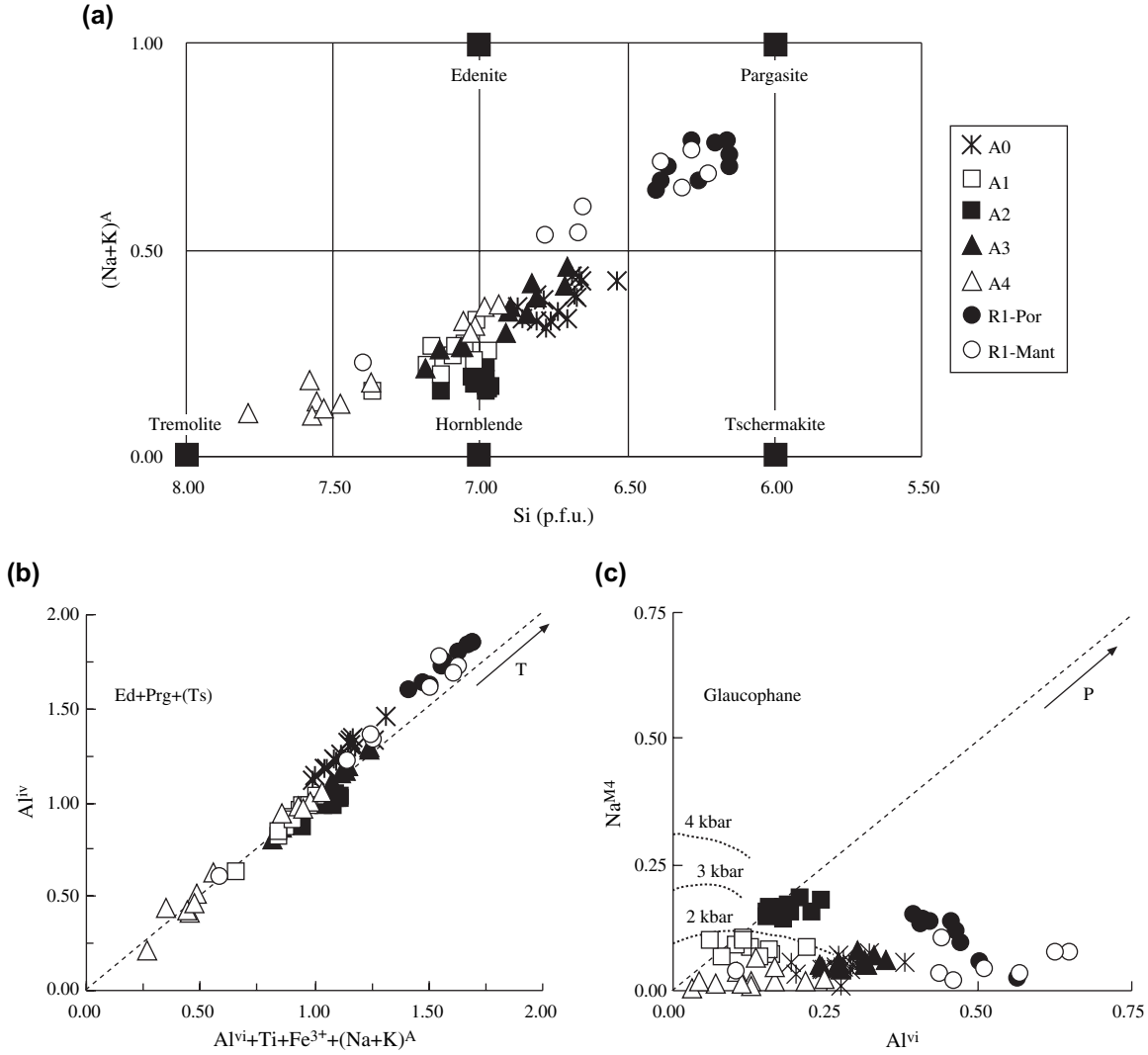

Fig. 4. (a) $(Na + K)^A$ vs. Si (p.f.u.) classification of calcic amphiboles from the studied samples (Pe-Piper, 1988). (b) and (c) Relative influence of different coupled substitutions on the compositional variability of the studied amphiboles (Spear, 1981). (b) Al^{iv} vs. $Al^{vi} + Fe^{3+} + Ti + (Na + K)^A$ plot: ideal substitution mechanism proposed by Robinson et al. (1971) is depicted by a 1:1 line that intersects at (0, 0); Increasing values along this line broadly indicates increasing temperature (see the text for further discussion). (c) Na^{M4} vs. Al^{vi} plot: ideal glaucophane substitution is indicated by a 1:1 line that intersects at (0, 0); increasing values along this line approximates a pressure increase (see the text for further discussion). Isobarometric lines are deduced from the calibration by Brown (1977) assuming Al^{vi} approximates 1/5 Al^{iv} in the studied amphiboles (see Table 2).

axis/angle pairs can be measured easily from EBSD data and provide useful additional microstructural and petrofabric information (e.g. Wheeler et al., 2001). In this study, neighbour-pair (also known as correlated) misorientation analyses have been performed on samples which are representative of the three considered rock types: A2 (Acebuches banded amphibolites), A3 (Acebuches mylonitic metabasites) and R1 (El Rellano amphibolite).

The misorientation angle distributions of samples A2, A3 and R1 in general tend towards platykurtic and hence are close to the theoretical random distribution (Fig. 6). However, samples A3 and R1 exhibit relatively large frequencies for small misorientation angles (n.b. sample A1 exhibits a similar but much less pronounced effect). In the case of sample A3, these higher frequencies continue up to a misorientation angle of ~30° but for sample R1 there is an abrupt change at ~15°. The majority of small misorientation angles in sample R1 are associated with subgrain boundaries in coarse-grained porphyroclasts (Fig. 6c).

Given that for most misorientation angles there is little difference compared with the random case, no specific relationships are expected between misorientation axis/angle pairs and specific crystallographic orientations. Furthermore, no specific relationship is observed between the small misorientation angles and crystallographic directions for the Acebuches metabasites samples (samples A2 and A3, Fig. 7a,b). However, a slight correlation is observed between small misorientation angles (i.e. <15°) and the [001] crystallographic direction for sample R1 (Fig. 7c). This relationship is particularly common for the porphyroclasts cores (Fig. 7d); although no misorientation axis/angle pairs with angles larger than 20° have been found in the porphyroclasts cores. No correlation between misorientation pairs and crystallographic directions is observed beyond 35° misorientation angle.

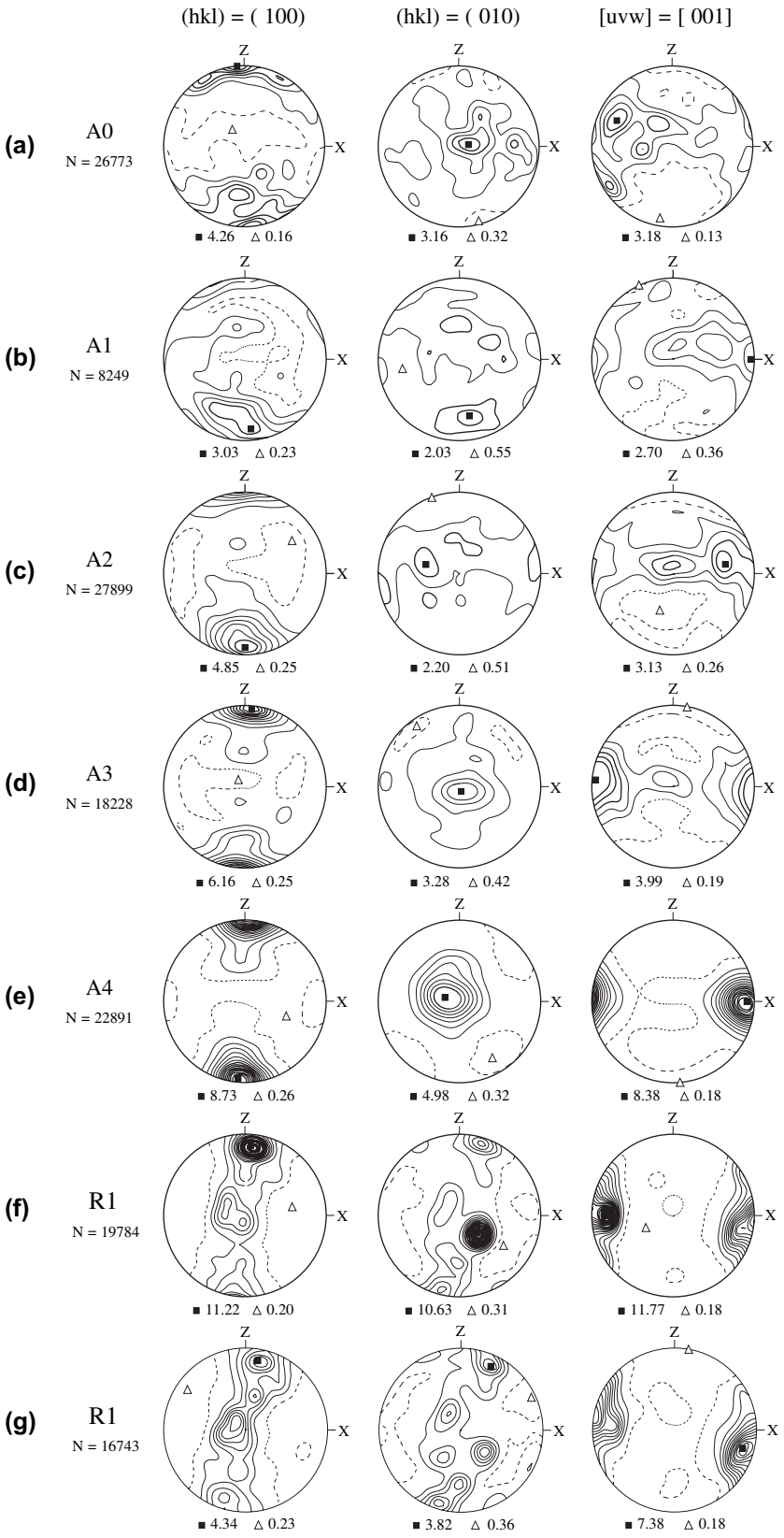

Fig. 5. Lower hemisphere, non-polar, equal-area projections of (100) and (010) planes, and [001] direction of the studied amphiboles: contour intervals, 0.5 multiples of uniform distribution (mud); broken line, minimum (0.5 mud) contour interval; black squares and white triangles are maximum and minimum densities respectively; N, number of measurements. Samples are: (a) A0, (b) A1, (c) A2, (d) A3, (e) A4, (f) R1 (including porphyroclasts coarser than 5 mm), (g) R1 (excluding porphyroclasts coarser than 5 mm).

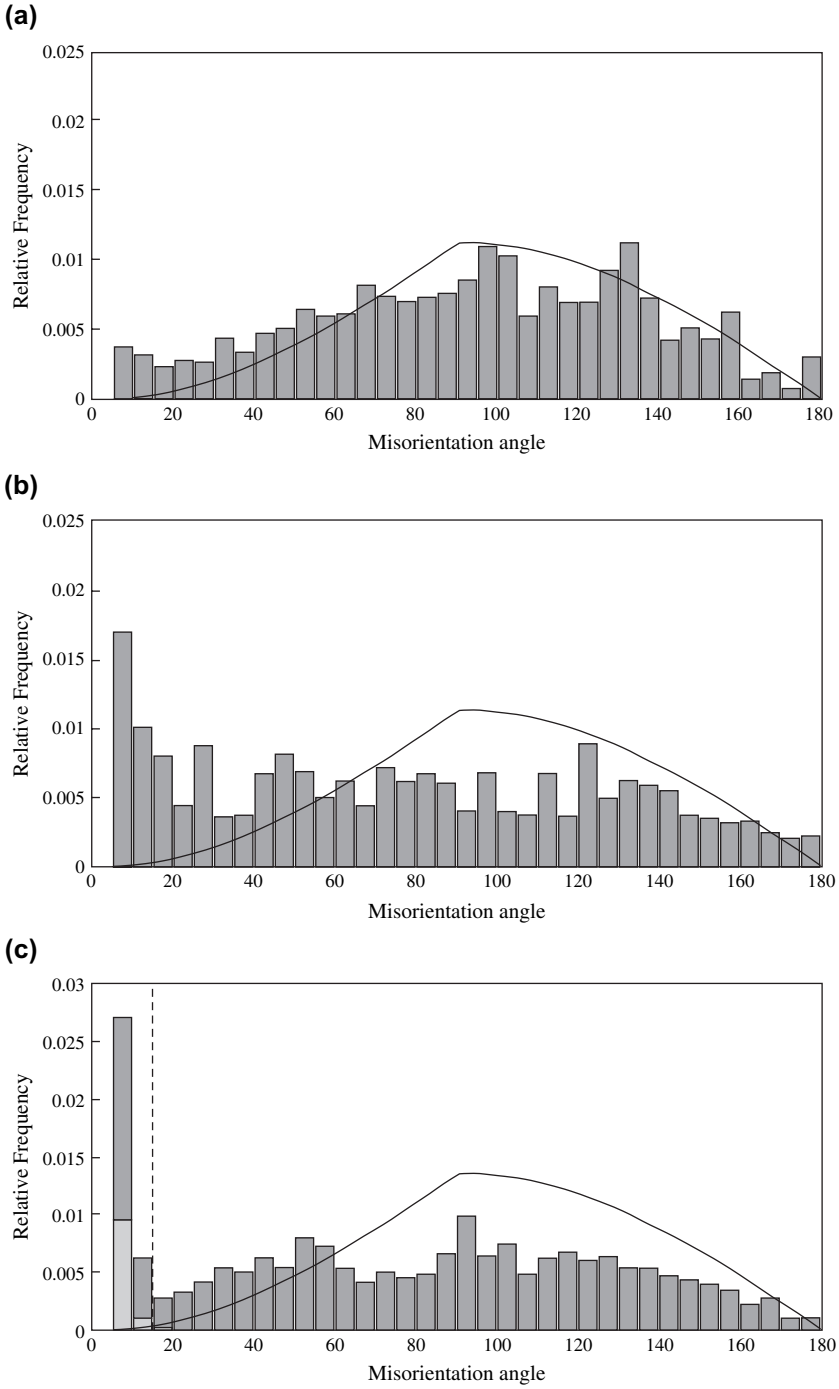

Fig. 6. Neighbour-pair misorientation angle frequency distributions for samples: (a) A2 (Acebuches banded amphibolite); (b) A3 (Acebuches mylonitic amphibolite); and (c) R1 (El Rellano amphibolite). In (c), dark grey bars correspond to fine mantle grains (grain size <400 μm) whereas light grey bars correspond to porphyroclasts cores (grain size >400 μm). Dashed line in sample R1 (c) coincides with misorientation angle of 15° and marks a change in the misorientation frequency distribution (see the main text). The theoretical random distribution curve for amphibole is shown for comparative purposes.

5. Discussion: LPO development in amphiboles deformed under LP conditions

5.1. Acebuches metabasites

LPO of minerals have been traditionally interpreted as evidence for deformation by dislocation creep (e.g., Wenk, 1985). However, no microfabric evidence of crystal plastic deformation (i.e., undulose extinction, deformation bands, subgrains, crystallographic controlled misorientation axes, etc.) has been found in amphiboles from the Acebuches metabasites. These amphiboles display a strong correlation between LPO and SPO strength (compare Fig. 3a,b with Fig. 5a–e). In effect, amphiboles from the banded amphibolites define

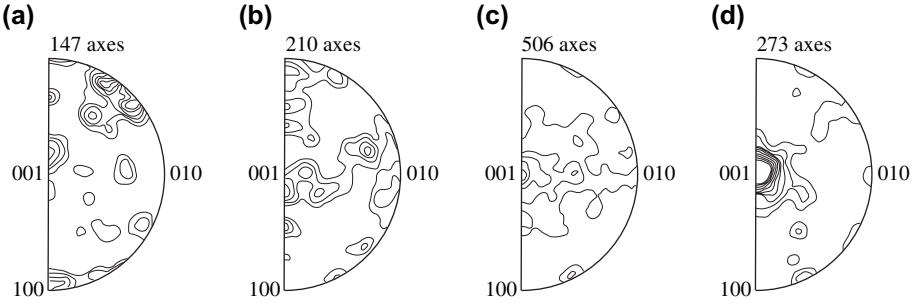

Fig. 7. Upper hemisphere, equal area inverse pole figures of misorientation axis/angle pair for angles lower than 10° in different samples. The number of axes corresponding to misorientation angles lower than 10° is shown at the top of each pole figure. Contour intervals are 1 multiple of uniform distribution (mud). Half width is 10° and cluster size is 0°. Minimum density is 0.00. (a) 7875 data points from sample A2 (Acebuches banded amphibolite). Maximum density equals 75.3. (b) 2512 data points from sample A3 (Acebuches mylonitic amphibolite), with a maximum density of 97.04. (c) 5416 data points of mantle grains (finer than 400 μm) from the El Rellano amphibolite (sample R1). Maximum density is 93.47. (d) Porphyroclasts (grains coarser than 400 μm, 304 data points) from sample R1 (El Rellano amphibolite). Maximum density is 126.56.

a weak SPO, with small aspect ratios and a weak foliation (Fig. 3a), and this correlates with a weak LPO (Fig. 5a–c). On its turn, the mylonitic metabasites present a strong SPO characterised by larger aspect ratios and a well-defined foliation (Fig. 3b) that correlates with a strong LPO (Fig. 5d,e). Moreover, in the mylonitic metabasites the orientation of the long axes lies subparallel to the orientation of [001] crystallographic axes. These features suggest the LPO displayed by the Acebuches metabasites could have formed by rigid body rotation of elongate amphibole grains in a less viscous plagioclase matrix. This mechanism is considered to play an important role in LPO development in clinoamphiboles (Brodie and Rutter, 1985; Shelley, 1994; Berger and Stünitz, 1996; Baratoux et al., 2005).

Rigid body rotation could explain the observed differences between the fabric of the banded amphibolites (samples A0–A2) and that of the mylonitic metabasites (samples A3 and A4). The small aspect ratio of amphiboles from the banded amphibolites means that there is a small difference between the long and the intermediate lengths of amphibole prisms. During the AM-D_1 deformation phase, amphibole grains rotated towards the XY plane of the finite strain ellipsoid (e.g., Passchier and Trouw, 1996, and references therein) such that their (100) planes became parallel to and hence physically define the foliation (Fig. 5a–c). However, due to the only slight difference between the [010] and [001] dimensions, neither became preferentially aligned with the macroscopic stretching direction. Rather, they tended to become scattered within the foliation plane (Fig. 5a–c). This process would account also for the scarcity of stretching lineations in the banded amphibolites. In contrast, amphiboles from the mylonitic metabasites display a steep increase in aspect ratio towards the footwall of the SISZ (Fig. 3b, Table 1; see also Díaz Aspiroz and Fernández, 2003) and consequently the [001] direction rotated preferentially towards the stretching direction (X) and defines the penetrative stretching lineation observed in these rocks (Fig. 5d,e). Furthermore, the banded amphibolites fabric developed during the AM-D_1 deformation from an isotropic rock (a basalt) whereas the mylonitic metabasites fabric formed during the AM-D_2 deformation within the SISZ from an anisotropic rock, probably the banded amphibolites (Díaz Aspiroz and Fernández, 2003), which had a definite fabric (Fig. 5a–c). This difference could account also for the stronger LPO observed in the mylonitic metabasites. However, if AM-S_2 developed over an earlier foliation (i.e., AM-S_1) and both were subparallel (Fig. 1), it is likely (see Passchier and Trouw, 1996 p. 70, and Passchier, 1997) that AM-D_2 involved coaxial flow that caused elongate amphibole prisms to rotate towards the fabric attractors. This observation is in agreement with the transpressional nature of the SISZ (Díaz Aspiroz and Fernández, 2005).

The AM-D_2 deformation that formed the SISZ involved drastic grain-size reduction of amphiboles from the mylonitic metabasites (Díaz Aspiroz and Fernández, 2003), which could be due to cataclastic flow. Straight grain boundaries parallel to the long axes of the amphibole prisms could be explained by fracturing along both the (100) and (010) cleavage planes (Fig. 2c,d). A similar process has been described by Berger and Stünitz (1996) and it could be responsible, at least in part, for the progressive increase in the aspect ratio of these amphiboles. However, the long axis length must have been reduced also by fracturing normal to [001] (Fig. 2e), a feature first recognised by Allison and La Tour (1977) to explain drastic grain-size reduction in amphiboles. Cataclasis in the Acebuches metabasites could have been related to mechanical interaction between amphibole grains during rigid body rotation. The modal proportion of amphibole in these rocks is 30–50% (Table 1), which means that mechanical interactions between amphibole grains are greatly expected. These interactions would cause rigid body rotation of single amphibole grains to block or slow down (cf. Ildefonse et al., 1992). As a weak fabric is expected under such circumstances (Ildefonse et al., 1992), the strong SPO and LPO shown by these amphiboles (Figs. 3b and 5d,e) suggest that rigid body rotation continued somehow after blocking. When an amphibole grain was blocked, fracturing and subsequent rotation of newly formed disconnected fragments probably occurred. This rotation-interaction-blocking-fracturing-rotation process would have been repeated several times, progressively causing: (1) reduction of the size of the newly formed amphibole fragments

(i.e., reducing the overall grain-size); and (2) strengthening of the amphibole SPO and LPO.

Normally, small-angle misorientations between neighbouring lattices, a feature observed in sample A3 (Figs. 6b and 7b) would suggest recovery or subgrain rotation recrystallization but the lack of any preferred relationship between the misorientation axes and sample crystallography argues against these processes. However, cataclasis of individual large parental amphibole grains would tend also to produce fragments with initially similar crystallographic orientations and hence small-angle misorientation relationships (e.g., Jiang et al., 2000). Furthermore, as the rotation that produces the misorientation between adjacent grain fragments occurs after cataclasis, it is unlikely to be crystallographically controlled, although it may reflect the (local) kinematic and/or strain regime, probably clustering about the vorticity vector.

Apart from rigid body rotation and cataclastic flow, the amphiboles from the mylonitic metabasites could have been affected also by dissolution-precipitation creep, which would account for their chemical heterogeneity (Fig. 4; see Watts and Williams, 1983; Berger and Stünitz, 1996) and also it could have reinforced their LPO (cf. Bons and den Brok, 2000). The latter would have strengthened the differences between the LPO of these rocks and that of the banded amphibolites. The Acebuches metabasites show nearly constant chemical and modal compositions (Table 1, see also Castro et al., 1996) and were deformed under constant, low-pressure (<4 kbar) metamorphic conditions (Fig. 4, see also Castro et al., 1996; Díaz Aspiroz et al., 2006). Therefore, the observed differences in the rheological behaviour of the banded amphibolites and the mylonitic metabasites could be related to differences in temperature and, perhaps, fluid content although, as yet unrecognised differences in deformation styles between the poorly studied AM-D_1 and AM-D_2 events also could be significant. Usually, cataclastic flow and solution transfer processes appear to be favoured by both low temperatures and hydrous systems (Wilks and Carter, 1990; Berger and Stünitz, 1996). The mylonitic metabasites were deformed under lower temperatures than the banded amphibolites (Table 1, see also Castro et al., 1996; Díaz Aspiroz, 2006). In addition, infiltration of fluids into the SISZ would have been favoured by cataclastic flow (see Matthäi and Roberts, 1997), considering also that fluid flow is usually focused within fault zones (e.g., Strayer et al., 2001 and references therein). The presence of fluids in the mylonitic metabasites would have enhanced the hydration down-grade metamorphic reactions observed in these rocks (Díaz Aspiroz, 2006) and perhaps provoked switching from cataclasis to dissolution-precipitation creep as the main deformation mechanism. A similar process has been proposed by Imon et al. (2002) in lower-amphibolite facies metabasites from the Ryoke belt.

5.2. El Rellano amphibolite

Amphiboles from the El Rellano amphibolites show a weak SPO (Fig. 3c,d) and a strong LPO (Fig. 5f,g). Accordingly, the observed distribution of [001] directions in the El Rellano amphibolites, which is aligned close to the X-direction, does not correlate with the alignment of the long-axes of prismatic grains, as is observed in the Acebuches metabasites and, thus, rigid body rotation can be dismissed. Also, the core and mantle structures defined by amphiboles from the El Rellano amphibolites (see Section 5.1 and Fig. 2g,h) are different from core and mantle structures attributed to cataclastic flow (see Nyman et al., 1992; Berger and Stünitz, 1996; Baratoux et al., 2005). In addition, there is a strong correlation between small-angle misorientation axes and the [001] crystallographic direction (Fig. 7c,d), which is incompatible with a cataclastic process. The observed features of the El Rellano amphibolites (undulose extinction, subgrains, crystallographic controlled low-angle boundaries, etc.) suggest (according to Schmid, 1982; Tullis and Yund, 1987; Hirth and Tullis, 1992; Lafrance and Vernon, 1993; Nyman and Tracy, 1993; Passchier and Trouw, 1996, and references therein) the LPO development in these amphiboles was mainly due to dislocation creep accommodated by subgrain rotation dynamic recrystallization, which probably concentrated at the rims of porphyroclasts. The amphibole LPO from the El Rellano amphibolite (Fig. 5f,g) is consistent with dislocation creep on (100)[001] and (010) [001] slip-systems, which is in accordance with the crystal slip systems reported for amphiboles deformed at high temperatures (Dollinger and Blacic, 1975; Rooney et al., 1975; Morrison-Smith, 1976; Biermann and van Roermund, 1983; Skrotzki, 1990). Dynamic recrystallization may have been chemically enhanced (e.g., Yund and Tullis, 1991; Berger and Stünitz, 1996), as significant chemical differences have been found between porphyroclast cores and mantle grains (Fig. 4a,b).

The El Rellano amphibolites were deformed, as the Acebuches banded amphibolites, at low-pressures (4–6 kbar) under anhydrous conditions (Díaz Aspiroz et al., 2006). However, the higher temperatures of the El Rellano amphibolites would have favoured amphibole deformation by crystal plasticity instead of rigid body rotation and cataclastic flow (e.g., Wilks and Carter, 1990; Berger and Stünitz, 1996).

5.3. Amphibole misorientation analysis

The neighbour-pair misorientation data for amphiboles from the El Rellano amphibolites (Figs. 6c and 7c,d) emphasise a potential problem and/or lack of understanding in misorientation analysis. The data indicate that the [001] direction is the favoured misorientation axis, in which case subgrain rotation recrystallization presumably occurred around tilt boundaries with [001] parallel to the (100) and (010) slip-planes (see Lloyd et al., 1997). In principle, a misorientation axis cannot be parallel to a direction of crystal slip as the two directions must be mutually perpendicular (e.g., Lloyd et al., 1997). However, the slip systems recognised for amphibole (see above) typically have [001] as the slip direction and the LPO reported here (Fig. 5) support this observation. Although the rotation axis for crystal slip (e.g. Lloyd and Freeman, 1994) and the misorientation axis are only parallel in the case of ideal tilt boundaries and are perpendicular for ideal twist boundaries, where the

latter is parallel to the slip plane normal direction, in both situations the misorientation axis is always perpendicular to the slip direction (Lloyd et al., 1997). This potential paradox may be resolved by recognising the cumulative impact of the operation of more than one slip system. If two or more slip systems combine to produce the overall LPO and are responsible also for the misorientation between adjacent grains, they will tend to form general boundaries with both tilt and twist components. In such cases the observed misorientation axis will be the (weighted) average of the ideal misorientation axes for the individual slip systems (see Lloyd, 2004). Thus, an apparent [001] misorientation axis could represent in practice the average of a number of different slip systems. This situation indicates that there is much to learn still about the crystal plastic deformation of amphiboles in particular and misorientation analysis in general.

5.4. Rheological constraints on amphibole LPO development in biminerallic metabasites

All of the metabasite samples considered in this contribution are typically biminerallic, consisting of amphibole and plagioclase in varying proportions. In such two-phase aggregates with different viscous strengths strain tends to be apportioned depending on: (1) strength contrast; (2) relative proportions of each phase; and (3) rock structure (Handy, 1994; Holyoke and Tullis, 2006, and references therein). The modal plagioclase/amphibole proportion is much lower in the El Rellano amphibolite than in the Acebuches banded amphibolites (i.e., 37/63 compared with 53–61/39–47, Table 1). Moreover, the El Rellano amphibolite displays a compositional layering defined by plagioclase-rich and amphibole-rich layers. Such differences in modal composition and structure could result in contrasting rheologies between the Acebuches and the El Rellano amphibolites.

Following Handy (1994), the Acebuches metabasites present an interconnected weak layer (IWL) structure in which plagioclase represents the weak phase. As plagioclase and amphibole exhibit a high strength contrast, strain partitioning between them is expected to have been high (for a detailed discussion of the effects of phase strength contrast on strain partitioning see Tullis and Wenk, 1994 and Holyoke and Tullis, 2006). Consequently, in the Acebuches metabasites strain should have concentrated on the weak phase (plagioclase), within which the strong phase (amphibole) rotated rigidly. The presence of only rare internal strain features in amphiboles suggesting that stress within those grains was low supports such a strain partitioning (cf. Handy, 1994). A similar process has been suggested previously for metabasites deformed under upper amphibolite facies conditions by Baratoux et al. (2005).

The El Rellano amphibolite is a banded mylonite formed by interconnected layers of weak plagioclase alternating with strong hornblende layers, which resulted from dynamic recrystallization of very coarse-grained plagioclases and hornblendes from the pegmatitic protolith. This type of structure has been previously interpreted as characteristic of high strains (e.g., Baratoux et al., 2005) and suggests also low strength contrast between plagioclase and hornblende (Handy, 1994). As experimental studies (Tullis and Wenk, 1994; Holyoke and Tullis, 2006) show that strain partitioning in polyphase rocks is favoured by high strength contrast, it is expected therefore that hornblende layers in the El Rellano amphibolite absorbed part of the total strain. The experiments of Tullis and Wenk (1994) and Holyoke and Tullis (2006) indicate that whilst the presence of isolated weak phases within strong framework structures favour localised brittle deformation of the strong phase, ductile behaviour of the strong phase is more likely to occur in monominerallic aggregates. Furthermore, other authors (Brodie and Rutter, 1985; Kruse and Stünitz, 1999) suggest that layers of pure hornblende are likely to deform by crystal plasticity under high-temperature conditions. Thus, the higher deformation temperatures and the presence of monominerallic (>90%) hornblende layers together explain the dislocation creep features observed in the amphiboles of the El Rellano amphibolite. Considering the deformation temperatures registered by the El Rellano amphibolite and the low influence of pressure in the rheological behaviour of amphibolites (e.g., Wilks and Carter, 1990), the rheological behaviour of amphiboles from the El Rellano amphibolite could reflect the rheology of amphiboles from a lower continental crust at high temperature conditions.

6. Conclusions

Metabasites from the Aracena metamorphic belt (AMB), SW Spain, were deformed under low-pressure (<6 kbar) metamorphic conditions at temperatures ranging from 650 to 970 °C. Based on textural and metamorphic features, three different metabasites have been distinguished: (1) fine-grained mylonitic Acebuches metabasites (samples A3, A4; T = 650–720 °C); (2) medium-to-coarse-grained banded Acebuches amphibolites (samples A0, A1, A2; T = 750–825 °C); and (3) fine-to-coarse grained mylonitic El Rellano amphibolites (sample R1; T = 840–970 °C).

Clinoamphiboles from the mylonitic Acebuches metabasites show a wide compositional range within the magnesio-hornblende compositional field. They have large aspect ratios, a strong SPO and display fracturing parallel to (100) and (010) cleavage planes and also normal to the [001] axis. Clinoamphiboles from the banded Acebuches amphibolites are magnesio-hornblendes with very slight compositional differences. They appear as prisms with small aspect-ratios that exhibit weak fracturing and define a weak SPO. Neither the Acebuches metabasites nor the banded amphibolites show microstructures indicative of crystal plastic deformation. Clinoamphiboles from the mylonitic the El Rellano amphibolite are mostly alkali-rich (pargasite to edenite) in composition. They appear as porphyroclasts with core and mantle structure showing a weak SPO. Cores often show undulose extinction and bent cleavage planes. Mantles are polygonised aggregates of regularly-shaped subgrains and grains with uniform size, small aspect ratios and straight or slightly curved boundaries. Subgrain boundaries at the margin of the cores are

optically distinguishable and pass laterally into larger-angle grain boundaries. Also, a gradual transition from subgrains aggregates to small mantle grains aggregates is observed.

The clinoamphiboles exhibit distinctive but different LPO, as determined by SEM/EBSD. In the mylonitic Acebuches metabasites, the well-developed LPO is characterised by (100) planes lying parallel to the foliation (XY) planes, (010) planes lying parallel to the XZ plane, and the [001] direction parallel to the X-direction. In the banded Acebuches amphibolites, LPO are less well developed and more varied, with (100) planes lying subparallel to the foliation plane, (010) planes showing a wide range of orientations, and the [001] directions tending to define a great circle girdle around Z. The mylonitic El Rellano amphibolite display strong LPO characterised by (100) and (010) planes defining a great circle girdle around the X-direction and a strong preferred orientation of the [001] directions slightly inclined in a clockwise sense with respect to the X-direction. In addition, misorientation analysis indicates that small misorientation angles are associated with subgrain boundaries in porphyroclasts and are correlated with the [001] crystallographic direction.

The amphibole LPO are attributed to different deformation mechanisms in the three rock types, which resulted from differences in deformation temperatures, fluid content, rock structure and phase-strength contrasts. The LPO of both the mylonitic and banded amphibolites Acebuches metabasites are due mainly to rigid body rotation of amphibole prisms within a weaker plagioclase matrix. Medium deformation temperatures, an interconnected weak layer structure and a high phase strength-contrast between plagioclase (weak phase) and clinoamphibole (strong phase) would account for this process. In addition, lower temperatures and the presence of fluids during deformation of the mylonitic Acebuches metabasites explain why these rocks were affected also by dissolution-precipitation creep and cataclastic flow, the latter resulting in increasing aspect-ratio and drastic grain size reduction. The LPO of the mylonitic El Rellano amphibolite is attributed to dislocation creep accommodated by recovery and subgrain rotation dynamic recrystallization, which were favoured by higher temperatures affecting monominerallic hornblende layers. As such, the El Rellano amphibolites may be representative of amphibole behaviour in a lower continental crust at high temperature conditions.

Acknowledgments

This study has received financial support by the Spanish Ministry of Science and Technology (projects PB94-1085, BTE2003 – 05057 – CO2 – 02, CGL2006-08638/BTE and CSD2006-00041). The SEM/EBSD facility at the University of Leeds was part funded by UK NERC grant GR9/3223. We wish to acknowledge the use of the UK EPSRC Chemical Database Service at Daresbury and the Cambridge Structural Database System. Thorough reviews by T. Okudaira and T. La Tour greatly improved this manuscript. MD thanks P. Cordier, D. Mainprice and D. Tatham for stimulating discussions.

References

Allen, F.H., 2002. The Cambridge Structural Database: a quarter of a million crystal structures and rising. Acta Crystallographica B58, 380–388.

Allison, I., La Tour, T.E., 1977. Brittle deformation of hornblende in a mylonite: a direct geometrical analogue of ductile deformation by translation gliding. Canadian Journal of Earth Sciences 14, 1953–1958.

Babaie, H.A., La Tour, T.E., 1994. Semibrittle and cataclastic deformation of hornblende-quartz rocks in a ductile shear zone. Tectonophysics 229, 19–30.

Baratoux, L., Schulmann, K., Ulrich, S., Lexa, O., 2005. Contrasting microstructures and deformation mechanisms in metagabbro mylonites contemporaneously deformed under different temperatures (c. 650 °C and c. 750 °C). In: Gapais, D., Brun, J.P., Cobbold, P.R. (Eds.), Deformation Mechanisms, Rheology and Tectonics: from Minerals to the Lithosphere. Geological Society, London, Special Publications, vol. 243, pp. 97–125.

Bard, J.P., 1969. Le métamorphisme régional progressif de Sierra de Aracena en Andalousie occidentale (Espagne). Ph.D thesis, University of Montpellier.

Bard, J.P., Moine, B., 1979. Acebuches amphibolites in the Aracena hercynian metamorphic belt (southwest Spain): geochemical variations and basaltic affinities. Lithos 12, 271–282.

Berger, A., Stünitz, H., 1996. Deformation mechanisms and reaction of hornblende: examples from the Bergell tonalite (Central Alps). Tectonophysics 257, 149–174.

Biermann, C., 1981. (100) Deformation twins in naturally deformed amphiboles. Nature 292, 621–633.

Biermann, C., van Roermund, H.L.M., 1983. Defect structures in naturally deformed clinoamphiboles-a TEM study. Tectonophysics 95, 267–278.

Blundy, J.D., Holland, T.J.B., 1990. Calcic amphibole equilibria and a new amphibole-plagioclase geothermometer. Contributions to Mineralogy and Petrology 104, 208–224.

Bons, P.D., den Brok, B.W.J., 2000. Crystallographic preferred orientation development by dissolution precipitation creep. Journal of Structural Geology 22, 1713–1722.

Brodie, K.H., Rutter, E.H., 1985. On the relationship between deformation and metamorphism, with special reference to the behaviour of basic rocks. In: Thompson, A.B., Rubie, D.C. (Eds.), Metamorphic Reactions: Kinetics, Textures and Deformation. Springer-Verlag, New York, pp. 138–179.

Brown, E.H., 1977. The crossite content of Ca-amphibole as a guide to pressure of metamorphism. Journal of Petrology 18, 53–72.

Castro, A., Fernández, C., de la Rosa, J.D., Moreno-Ventas, I., Rogers, G., 1996. Significance of MORB-derived Amphibolites from the Aracena Metamorphic Belts, Southwest Spain. Journal of Petrology 37, 235–260.

Castro, A., Fernández, C., El-Hmidi, H., El-Biad, M., Díaz, M., de la Rosa, J.D., Stuart, F., 1999. Age constraints to the relationships between magmatism, metamorphism and tectonism in the Aracena metamorphic belt, southern Spain. International Journal of Earth Sciences 88, 26–37.

Chao, E.C.T., 1967. Shock effects in certain rock forming minerals. Science 156, 192–202.

Crespo-Blanc, A., Orozco, M., 1988. The Southern Iberian Shear Zone: a major boundary in the Hercynian folded belt. Tectonophysics 148, 221–227.

Cumbest, R.J., Drury, M.R., van Roermund, H.L.M., Simpson, C., 1989. Dynamic recrystallization and chemical evolution of clinoamphiboles from Senja, Norway. Contributions to Mineralogy and Petrology 101, 339–349.

Dias, R., 2004. Finite Strain Tensor (FIST 2.2).

Díaz Aspiroz, M., 2006. Evolución tectono-metamórfica del dominio de alto grado de la banda metamórfica de Aracena. Serie Nova Terra, vol. . 30. Laboratorio Xeolóxico de Laxe, La Coruña.

Díaz Aspiroz, M., Fernández, C., 2003. Characterization of tectono-metamorphic events using crystal size distribution (CSD) diagrams. A case study from the Acebuches metabasites (SW Spain). Journal of Structural Geology 25, 935–947.

Díaz Aspiroz, M., Fernández, C., 2005. Kinematic analysis of the Southern Iberian shear zone and tectonic evolution of the Acebuches metabasites (SW Variscan Iberian Massif). Tectonics, 24, TC3010, doi:10.1029/2004TC001682.

Díaz Aspiroz, M., Fernández, C., Castro, A., 2003. Estructura y evolución tectónica del dominio continental de la banda metamórfica de Aracena (Macizo Ibérico meridional). Revista de la Sociedad Geológica de España 16, 167–184.

Díaz Aspiroz, M., Fernández, C., Castro, A., El-Biad, M., 2006. Tectono-metamorphic evolution of the Aracena metamorphic belt (SW Spain) resulting from ridge-trench interaction during Variscan plate convergence. Tectonics, 25, TC1001, doi:10.1029/2004TC001742.

Dollinger, G., Blacic, J.D., 1975. Deformation mechanisms in experimentally and naturally deformed amphiboles. Earth and Planetary Science Letters 26, 409–416.

Dupuy, C., Dostal, J., Bard, J.P., 1979. Trace element geochemistry of paleozoic amphibolites from SW Spain. Tschermak's Mineralogisch Petrographische Mitteilungen 26, 87–93.

Egydio-Silva, M., Vauchez, A., Bascou, J., Hippert, J., 2002. High-temperature deformation in the Neoproterozoic transpressional Ribera belt, southeast Brazil. Tectonophysics 352, 203–224.

Fletcher, D.A., McMeeking, R.F., Parkin, D., 1996. The United Kingdom Chemical Database Service. Journal of Chemical Information and Computer Sciences 36, 746–749.

Grapes, R.H., Graham, C.M., 1978. The actinolite-hornblende series in metabasites and the so-called miscibility gap: a review. Lithos 11, 85–97.

Hacker, B.R., Christie, J.M., 1990. Brittle/ductile and plastic/cataclastic transition in experimentally deformed and metamorphosed amphibolite. In: Duba, A.G., Durham, W.B., Handin, J.W., Wang, H.F. (Eds.), The Brittle-Ductile Transition in Rocks. AGU Geophysical Monograph, pp. 127–148.

Handy, M.R., 1994. Flow laws for rocks containing two non-linear viscous phases: a phenomenological approach. Journal of Structural Geology 16, 287–301.

Hirth, G., Tullis, J., 1992. Dislocation creep regimes in quartz aggregates. Journal of Structural Geology 14, 145–159.

Holland, T.J.B., Blundy, J.D., 1994. Non-ideal interactions in calcic amphiboles and their bearing on amphibole-plagioclase thermometry. Contributions to Mineralogy and Petrology 116, 433–447.

Holyoke, C.W., Tullis, J., 2006. Mechanisms of weak phase interconnection and the effects of phase strength contrast on fabric development. Journal of Structural Geology 28, 621–640.

Ildefonse, B., Launeau, P., Bouchez, J.L., Fernandez, A., 1992. Effect of mechanical interactions on the development of shape preferred orientations: a two-dimensional experimental approach. Journal of Structural Geology 14, 73–83.

Imon, R., Okudaira, T., Fujimoto, A., 2002. Dissolution and precipitation processes in the deformed amphibolites: an example from the ductile shear zone of the Ryoke metamorphic belt, SW Japan. Journal of Metamorphic Geology 20, 297–308.

Imon, R., Okudaira, T., Kanagawa, K., 2004. Development of shape- and lattice-preferred orientations of amphibole grains during cataclastic deformation and subsequent deformation by dissolution-precipitation creep in amphibolites from the Ryoke metamorphic belt, SW Japan. Journal of Structural Geology 26, 793–805.

Jiang, Z., Prior, D.J., Wheeler, J., 2000. Albite crystallographic preferred orientation and grain misorientation distribution in a low-grade mylonite: implications for granular flow. Journal of Structural Geology 22, 1663–1674.

Kirby, S.H., Kronenberg, A.K., 1987. Rheology of the lithosphere: selected topics. Reviews in Geophysics 25, 3177–3192.

Kretz, R., 1983. Symbols for rock-forming minerals. American Mineralogist 68, 277–279.

Kruse, R., Stünitz, H., 1999. Deformation mechanisms and phase distribution in mafic high-temperature mylonites from the Jotun Nappe, southern Norway. Tectonophysics 303, 223–249.

Lafrance, B., Vernon, R.H., 1993. Mass transfer and microfracturing in gabbroic mylonites of the Guadalupe igneous complex, California. In: Boland, J.N., Fitz Gerald, J.D. (Eds.), Defects and Processes in the Solid State: Geoscience applications, the McLaren Volume. Developments in Petrology, 4, pp. 151–167.

Leake, B.E., et al., 1997. Nomenclature of amphiboles: report of the subcommittee on amphiboles of the international mineralogical association commission on new minerals and mineral names. Mineralogical Magazine 61, 295–321.

Lloyd, G.E., 1987. Atomic number and crystallographic contrast images with the SEM: a review of backscattered electron techniques. Mineralogical Magazine 51, 3–19.

Lloyd, G.E., 2004. Microstructural evolution in a mylonitic quartz simple shear zone: the significant roles of dauphine twinning and misorientation. In: Alsop, G.I., Holdsworth, R.E., McCaffrey, K., Hand, M. (Eds.), Transports and Flow Processes in Shear Zones. Geological Society, London, Special Publications, vol. 224, pp. 39–61.

Lloyd, G.E., Freeman, B., 1994. Dynamic recrystallization of quartz under greenschist conditions. Journal of Structural Geology 16, 867–881.

Lloyd, G.E., Farmer, A.B., Mainprice, D., 1997. Misorientation analysis and the formation of subgrain and grain boundaries. Tectonophysics 279, 55–78.

Mainprice, D., 1990. An efficient FORTRAM program to calculate seismic anisotropy from the lattice preferred orientations of minerals. Computers and Geosciences 16, 385–393.

Mainprice, D., 2003. PFch5. http://www.isteem.univ-montp2.fr/TECTONOPHY/petrophysics/software/petrophysics_software.html.

Mainprice, D., Humbert, M., 1994. Methods of calculating petrophysical properties from lattice preferred orientation data. Survey Geophysics 15, 572–592.

Mainprice, D., Barruol, G., Ben Ismail, W., 2000. The seismic anisotropy of the Earth's mantle: from single crystal to polycrystal. Geophysical Monographs 117, 237–264.

Matthäi, S.K., Roberts, S.G., 1997. Transient versus continuous fluid flow in seismically active faults: an investigation by electric analogue and numerical modelling. In: Jamtveit, B., Yardley, B. (Eds.), Fluid Flow and Transport in Rocks: Mechanisms and Effects. Chapman & Hall, London, pp. 263–295.

Meissner, R., Rabbel, W., Kern, H., 2006. Seismic lamination and anisotropy of the Lower Continental Crust. Tectonophysics 416, 81–99.

Morrison-Smith, D.J., 1976. Transmission electron microscopy of experimentally deformed hornblende. American Mineralogist 61, 272–280.

Nyman, M.W., Tracy, R.J., 1993. Petrological evolution of amphibolite shear zones. Cheyenne Belt, south-eastern Wyoming, USA. Journal of Metamorphic Geology 11, 757–773.

Nyman, M.W., Law, R.D., Smelik, E.A., 1992. Cataclastic deformation for the development of core and mantle structures in amphibole. Geology 20, 455–458.

Passchier, C.W., 1997. The fabric attractor. Journal of Structural Geology 19, 113–127.

Passchier, C.W., Trouw, R.A.J., 1996. Microtectonics. Springer-Verlag, Berlin.

Pe-Piper, G., 1988. Calcic amphiboles of mafic rocks of the Jeffers Brook plutonic complex, Nova Scotia, Canada. American Mineralogist 73, 993–1006.

Quesada, C., Fonseca, P.E., Munha, J., Oliveira, J.T., Ribeiro, A., 1994. The Beja-Acebuches Ophiolite (Southern Iberia Variscan fold belt): Geological characterization and geodynamic significance. Boletín Geológico y Minero de España 105, 3–49.

Ranalli, G., Murphy, D.C., 1987. Rheological stratification of the lithosphere. Tectonophysics 132, 281–295.

Randle, V., 1993. The Measurement of Grain Boundary Geometry. Institute of Physics Publishing, Bristol, 169 pp.

Robinson, P., Ross, M., Jaffe, H.W., 1971. Compositions of the anthophyllite-gedrite series, comparisons of gedrite and hornblende, and the anthophyllite-gedrite solvus. American Mineralogist 56, 1005–1041.

Rooney, T.P., Riecker, R.E., Ross, M., 1970. Deformation twins in hornblende. Science 169, 173–175.

Rooney, T.P., Riecker, R.E., Gavasci, A.T., 1975. Hornblende deformation features. Geology 3, 364–366.

Rybacki, E., Dresen, G., 2004. Deformation mechanism maps for feldspar rocks. Tectonophysics 382, 173–187.

Schmid, S.M., 1982. Microfabric studies as indicators of deformation mechanisms and flow laws operative in mountain building. In: Hsü, K.J. (Ed.), Mountain Building Processes. Academic Press, London, pp. 95–110.

Shelley, D., 1994. Spider texture and amphibole preferred orientation. Journal of Structural Geology 16, 709–717.

Siegesmund, S., Helming, K., Kruse, R., 1994. Complete texture analysis of a deformed amphibolite: comparison between neutron diffraction and U-stage data. Journal of Structural Geology 16, 131–142.

Skrotzki, W., 1990. Microstructure in hornblende of a mylonitic amphibolite. In: Knipe, R.J., Rutter, E.H. (Eds.), Deformation Mechanisms, Rheology and Tectonics. Geological Society, London, Special Publications, vol. 54, pp. 321–325.

Skrotzki, W., 1992. Defect structures and deformation mechanisms in naturally deformed hornblende. Physica Status Solidi (a) 131, 605–624.

Spear, F.S., 1981. An experimental study of hornblende stability and compositional variability in amphibolite. American Journal Science 281, 697–734.

Spear, F.S., 1993. Metamorphic Phase Equilibria and Pressure-Temperature-Time Paths. Mineralogical Society of America, Washington, D.C.

Strayer, L.M., Hudleston, P.J., Lorig, L.J., 2001. A numerical model of deformation and fluid-flow in an evolving thrust wedge. Tectonophysics 335, 121–145.

Stünitz, H., 1993. Transition from fracturing to viscous flow in a naturally deformed metagabbro. In: Boland, J.N., Fitz Gerald, J.D. (Eds.), Defects and Processes in the Solid State: Geoscience Applications, the McLaren Volume. Developments in Petrology, 4, pp. 121–150.

Stünitz, H., Fitz Gerald, G.D., 1993. Deformation of granitoids at low metamorphic grade. II: Granular flow in albite-rich mylonites. Tectonophysics 223, 299–334.

Terry, M.P., Heidelbach, F., 2006. Deformation-enhanced metamorphic reactions and the rheology of high-pressure shear zones, Western Gneiss Region, Norway. Journal of Metamorphic Geology 24, 3–18.

Tullis, J., Wenk, H.R., 1994. Effect of muscovite on the strength and lattice preferred orientation of experimentally deformed quartz aggregates. Materials Science and Engineering. A, Structural Materials: Properties. Microstructure and Processing 175 (1–2), 209–220.

Tullis, J., Yund, R.A., 1987. Transition from cataclastic flow to dislocation creep of feldspar: mechanisms and microstructures. Geology 15, 606–609.

Watts, M.J., Williams, G.D., 1983. Strain geometry, microstructure and mineral chemistry in metagabbro shear zones: a study of softening mechanisms during progressive mylonitization. Journal of Structural Geology 5, 507–517.

Wenk, H.R. (Ed.). 1985. Preferred Orientation in Deformed Metals and Rocks. An Introduction to Modern Texture Analysis. Academic Press, New York.

Wheeler, J., Prior, D.J., Jiang, Z., Spiess, R., Trimby, P.W., 2001. The petrological significance of misorientation between grains. Contributions to Mineralogy and Petrology 141, 109–124.

Wilks, K.R., Carter, N.L., 1990. Rheology of some continental lower crustal rocks. Tectonophysics 182, 57–77.

Yund, R.A., Tullis, J., 1991. Compositional changes of minerals associated with dynamic recrystallization. Contributions to Mineralogy and Petrology 108, 346–355.